METALS AND MATERIALS International, Vol. 13, No. 6 (2007), pp. 479~482

Fabrication of MgO Whiskers on Metal-Coated Substrates by Heating MgB_2 Powders: Effects of Ag Layer Thickness

Hyoun Woo Kim*, Seung Hyun Shim, and Jong Woo Lee

School of Materials Science and Engineering, Inha University,
253, Yonghyeon-dong, Nan-gu, Incheon 402-751, Korea

A thermal evaporation approach was developed to synthesize single-crystalline MgO whiskers on silver (Ag) layer-coated Si substrates. Magnesium diboride (MgB_2) and oxygen (O_2) were used as Mg and O precursors, respectively. The synthetic process using a thinner Ag layer facilitated the growth of 1D whiskers, and the product mainly comprises film-like structures with thicker Ag layer thickness. X-ray diffraction and selected area electron diffraction pattern revealed that the whiskers were of a single-crystalline cubic structure of MgO. We also discuss the possible mechanism by which the thickness of the underlying Ag layer affects the resultant morphology of the MgO structures.

Keywords: MgO, whiskers, MgB_2, Ag layer

1. INTRODUCTION

The discovery of carbon nanotubes in 1991 [1] stimulated widespread interest in the synthesis of nanometer-sized forms of various materials [2-4]. With enhanced physical properties due to their decreased size, increased surface-to-volume ratio, and novel morphologies, one-dimensional (1D) nanomaterials can be applied as functional components for the fabrication of nanoscale electronic, optical, optoelectronic, electromechanical, and sensing devices [5]. Magnesium oxide (MgO) is a wide-band-gap insulator, and the electronic and optical properties of bulk MgO have been intensively investigated [6-8]. It has found many important applications including in catalysis, toxic waste remediation, and as additives in refractory, paint, and superconductor products [9-11]. In particular, 1D MgO nanostructures display a unique capability to pin magnetic flux lines within a high-temperature superconductor (HTSC). It was demonstrated that the incorporation of 1D MgO nanostructures as columnar defects into HTSCs can dramatically improve the HSTC performance at elevated temperatures or under intensive magnetic fields [12].

In this paper, MgO whiskers have been fabricated onto Ag-coated Si substrates. We have investigated the effect of Ag layer thickness on the morphology of the resulting product. Thermal evaporation of MgB_2 powders was carried out at a temperature of 900 °C. Additionally, we have reported a visible light emission from the as-synthesized MgO whiskers.

*Corresponding author: hwkim@inha.ac.kr

2. EXPERIMENTAL PROCEDURE

MgO whiskers were synthesized in a conventional tube furnace with a horizontal quartz glass tube [13]. The synthetic route can be described as follows. Commercial MgB_2 powders, employed as a source material, were put in an alumina boat. In order to fabricate Ag-coated Si substrates, Si was used as the starting material, onto which an Ag layer with a thickness in a range of approximately 7 nm to 32 nm was deposited by ion sputtering (Emitech, K757X). Since the authors believe that the formation of cluster-like Ag substrates is crucial for the fabrication of a whisker-like product, the Ag-coated substrates were thermally annealed at 300 °C for 30 min. With a vertical separation of about 10 mm, a piece of the substrate was placed on the top of the source materials with the Ag-coated side downwards. The quartz tube was inserted into a horizontal tube furnace. During the experiment, the furnace was maintained at a temperature of 900 °C with ambient gas ($Ar+O_2$) gas at a constant total pressure of 2 Torr. The typical percentages of O_2 and Ar partial pressure, respectively, were set to approximately 1.5 % and 98.5 %. After 2 h of evaporation, the substrate was cooled and subsequently removed from the furnace for structural and optical characterization.

A scanning electron microscope (SEM, Hitachi S-4200) was used to observe the overall morphology of the product. The structural properties of the as-grown products were

investigated using x-ray diffraction (XRD, X'pert MRD-Philips) with CuKα_1 radiation ($\lambda = 0.154056$ nm) with an incidence angle of 0.5°. For the selected area electron diffraction (SAED) analysis and energy-dispersive x-ray spectrometry (EDX) measurements, we have used a Philips CM-200 transmission electron microscope with 200 kV as the accelerating voltage. A transmission electron microscopy (TEM) sample was prepared by the following procedure: A small section of the whiskers was stripped off and dispersed in acetone with the aid of ultrasonic vibration for 20 min. A drop of this solution was then added to a copper microgrid covered by carbon. PL measurements were carried out using a He-Cd laser line (325 nm, 55 mW) as the excitation source at room temperature.

3. RESULTS AND DISCUSSION

The as-prepared products were characterized by XRD. The XRD pattern shown in Fig. 1 reveals the overall crystal structure of the product on an Ag-coated substrate. Miller indices are indicated on each diffraction peak. Apart from the peaks possibly originating from the Ag layer, all of the recognizable peaks can be indexed by their peak positions as reflecting a face-centered cubic structure of MgO with a lattice parameter of a = 0.421 nm, consistent with that of the bulk MgO crystal (JCPDS: 04-0829). We found that the XRD spectrum was not significantly dependent on the Ag layer thickness, revealing that the deposits are a crystalline MgO phase, regardless of the underlying Ag-layer thickness. In the present XRD measurements, the angle of the incident beam to the substrate surface was approximately 0.5° and the detector was rotated to scan the samples, minimizing the contribution from the Si substrate.

Figure 2(a) presents a typical low-magnification SEM image of the deposits on an Ag layer with a thickness of 7 nm,

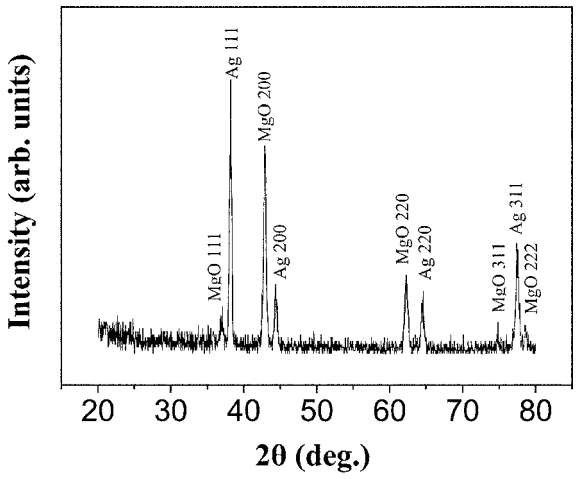

Fig. 1. Typical XRD pattern of the products, with an incidence angle of 0.5°.

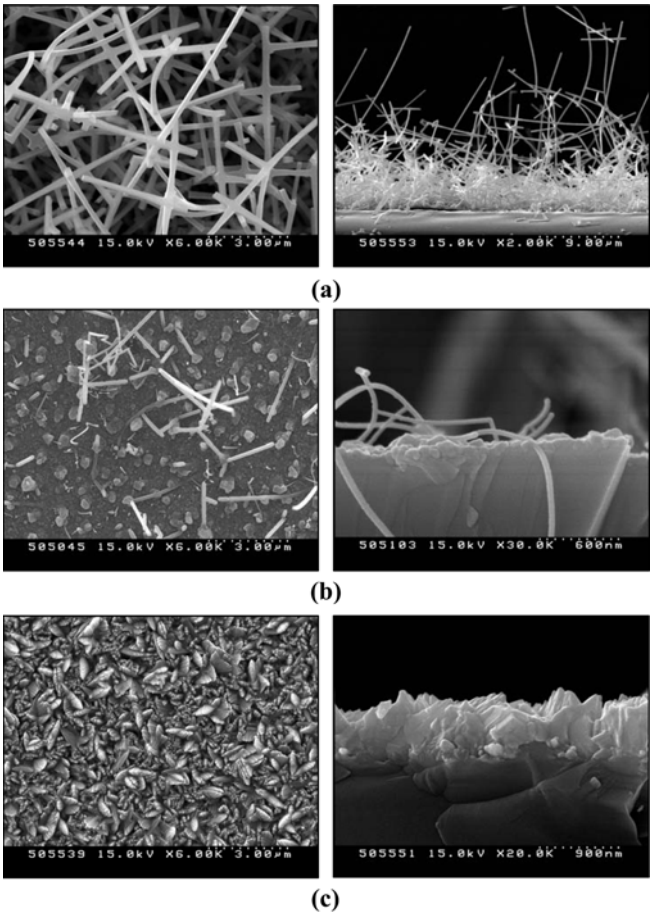

Fig. 2. Low-magnification SEM images of deposits on Ag layers with a thickness of (a) 7 nm, (b) 18 nm, and (c) 32 nm (Left: Top-view images; Right: Side-view images).

showing an agglomeration of 1D structures. The 1D structures have nearly uniform diameters along the length direction, with their geometrical shapes closely resembling solid rods. The whiskers have no nanoparticles at their tips. From a statistical analysis of many SEM images it is found that the whiskers have average diameters ranging from 100 to 300 nm. Figure 2(b) shows a SEM image of deposits on a 18 nm-thick Ag layer, revealing deposits comprised of film-like or cluster-like structures with some 1D structures. Figure 2(c) shows a SEM image of deposits on a 32 nm-thick Ag layer, indicating that the product mainly comprises flake-like or film-like structures.

Figure 3(a) shows a SEM image enlarging a tip region of a whisker, indicating that no catalyst particle is present at the tip. The individual whisker was further examined by TEM, and the inset in Fig. 3(a) shows an SAED pattern, recorded perpendicular to the whisker's long axis. The SAED pattern can be indexed as the [001] zone axis of crystalline MgO, revealing the single-crystalline nature of the whiskers. An EDX analysis indicated that the product consisted of only Mg and O elements, regardless of the position in the whis-

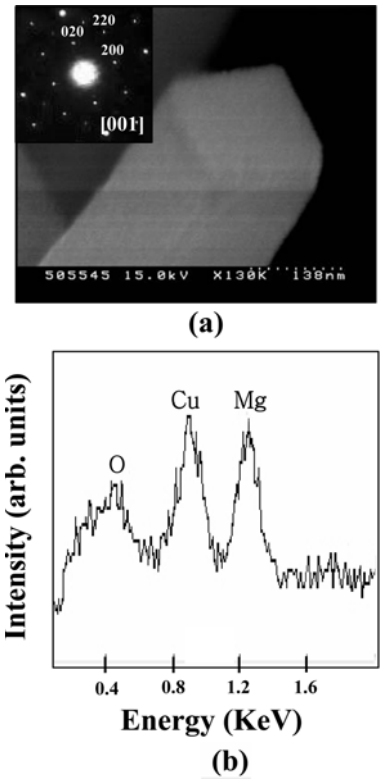

Fig. 3. (a) SEM image taken near the tip region of a whisker (inset: corresponding TEM-EDX pattern recorded along the [001] zone axis). (b) TEM-EDX spectrum of a single MgO whisker.

ker, i.e., from the stem to the tip. A typical EDX spectrum from the tip region of the whisker is shown in Fig. 3(b). The Cu component originated from the Cu TEM grid.

SEM observations indicated that only film-like structures were obtained when using a thicker Ag layer, whereas the main product was 1D whiskers in the case of using a thinner Ag layer. Similarly, our previous experiments indicated that the characteristics of an underlying gold (Au) layer affected the morphology of the final MgO structures [14]. Although predeposition annealing at a relatively low temperature of 300 °C was employed, and thus the annealing process itself is not expected to change the morphology of the Ag layer significantly, the subsequent evaporation step at a higher temperature of 900 °C may contribute to variation of the morphology of the Ag layer. We surmise that the formation of MgO 1D whiskers was suppressed by employing a thicker Ag layer, presumably because the Ag layer could not be transformed into sufficiently small Ag islands. Therefore, we project that Ag islands provide sites for the independent growth of 1D structures, while a wide Ag layer substrate with many nucleation sites, which was obtained from the thick Ag layer, promotes agglomeration of nuclei, producing cluster-like or film-like structures. Schematic illustrations of the product formation with Ag layer thicknesses of 7 nm and 32 nm during the evolution of nanowire growth with a nanoparticle at the tip are presented in Figs. 4(a) and (b), respectively.

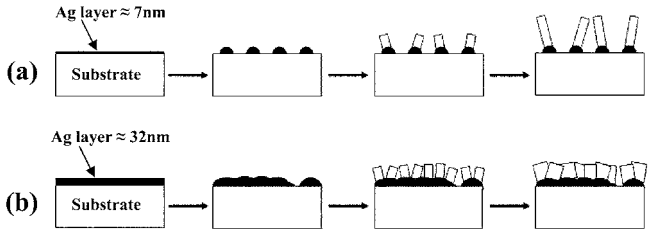

Fig. 4. Schematic illustrations of the product formation with Ag layer thicknesses of (a) 7 nm and (b) 32 nm.

Previous studies indicate that MgB_2 starts to decompose at ~800 °C and suggest that generated Mg vapor can react with the trace amount of O_2 contained in this system to generate MgO in the vapor phase [15]. The MgO vapor will ultimately deposit on the substrate. Several mechanisms for the growth of 1D nanostructures have been proposed, including vapor-liquid-solid (VLS), solution-liquid-solid (SLS), base-growth, and vapor-solid (VS) mechanisms. First, although Ag-coated substrates were employed, from the SEM and EDX analyses, there was no evidence that a catalyst is present at the tips of the structures. As a result, the catalyst-induced VLS and SLS mechanism can be ruled out. Accordingly, it is likely that the growth of MgO whiskers follows a mechanism similar to the VS mechanism and/or a base-growth mechanism.

Although the results are not presented in this paper, we have examined the room temperature PL spectra of the products on an Ag (7 nm-thick)-coated Si substrate. In order to obtain greater insight into the origin of PL emission, we have fitted the spectral feature with Gaussian functions. The best fit of the emission was obtained with two Gaussian functions, of which the peaks are centered at 2.37 and 2.89 eV, respectively. The peaks at 2.37 and 2.89 eV correspond to 524 nm in the blue-green region and 430 nm in the blue region, respectively. Similar blue emissions with peak positions around 2.81 eV to 2.83 eV [16,17] and around 2.64 eV [18] were previously reported in PL spectra from MgO nanostructures. In addition, a similar blue-green band centered at 2.45 eV has been observed from MgO nanobelts [19]. It is known that both the blue and blue-green light emissions can originate from defects in MgO, including oxygen vacancies [20], Mg vacancies, and interstitials. The defects induce the formation of new energy levels in the band gap of MgO. In this study, the high temperature evaporation process at 900 °C may have generated various structural defects, contributing to blue and blue-green emissions.

4. CONCLUSIONS

MgO whiskers were successfully synthesized on an Ag-

coated substrate via a thermal evaporation method, in which MgB_2 powders were heated to 900 °C. The thickness of the underlying Ag layer affects the resultant product morphology, and 1D whiskers were effectively produced by employing a relatively thin Ag layer. The obtained MgO whiskers, with diameters in a range of 100 nm to 300 nm, have a single-crystalline cubic structure. We have discussed the possible mechanism by which the thickness of the underlying Ag layer affected the resultant morphology of the MgO structures.

ACKNOWLEDGMENTS

This work was supported by a Korea Research Foundation Grant funded by the Korean Government (MOEHRD) (KRF-2007-521-D00216). The main calculations were performed by the supercomputing resource of the Korea Institute of Science and Technology Information (KISTI).

REFERENCES

1. S. Iijima, *Nature* **354**, 56 (1991).
2. J. Y. Kim, S. H. Kim, J. S. lee, K. W. Lee, and D. I. Kwon, *Met. Mater. -Int.* **12**, 219 (2006).
3. C. Y. Lim, S. Z. Han, and S. H. Lee, *Met. Mater. -Int.* **12**, 225 (2006).
4. J. Y. Chang, W. H. Park, A. A. Fraerman, and V. L. Mironov, *Met. Mater. -Int.* **11**, 415 (2005).
5. H. S. Yang, *Met. Mater. -Int.* **12**, 351 (2006).
6. G. P. Summers, T. M. Wilson, B. T. Jeffries, H. T. Tohver, Y. Chen, and M. M. Abraham, Phys. Rev. B **27**, 1283 (1983).
7. G. H. Rosenblatt, M. W. Rowe, G. P. Williams, Jr., R. T. Williams, and Y. Chen, *Phys. Rev. B* **39**, 10309 (1989).
8. J. L. Grant, R. Cooper, P. Zeglinski, and J. F. Boas, *J. Chem. Phys.* **90**, 807 (1989).
9. S. H. C. Liang and I. D. Gay, *J. Catal.* **101**, 293 (1986).
10. A. N. Copp, *Am. Ceram. Soc. Bull.* **74**, 135 (1995).
11. P. D. Yang and C. M. Lieber, *Science* **273**, 1836 (1996).
12. P. Yang and C. M. Lieber, *Science* **273**, 1836 (1996).
13. H. W. Kim, N. H. Kim, J. H. Myung, and S. H. Shim, *Phys. Stat. Sol. (a)* **202**, 1758 (2005).
14. H. W. Kim and S. H. Shim, *Chem. Phys. Lett*. **422**, 165 (2006).
15. Y. Yin, G. Zhang, and Y. Xia, *Adv. Funct. Mater.* **12**, 293 (2002).
16. F. L. Deepak, P. Saldanha, S. R. C. Vivekchand, and A. Govindaraj, *Chem. Phys. Lett.* **417**, 535 (2006).
17. K. P. Kalyanikutty, F. L. Deepak, C. Edem, A. Govindaraj, and C. N. R. Rao, *Mater. Res. Bull.* **40**, 831 (2005).
18. Y. Hao, G. Meng, C. Ye, X. Zhang, and L. Zhang, *J. Phys. Chem. B* **109**, 11204 (2005).
19. J. Zhang and L. Zhang, *Chem. Phys. Lett.* **363**, 293 (2002).
20. G. H. Rosenblatt. M. W. Rowe, G. P. Williams, Jr., R. T. Williams, and Y. Chen, *Phys. Rev. B* **39**, 10309 (1989).